Temporal Profile of Kynurenine Pathway Metabolites in a Rodent Model of Autosomal Recessive Polycystic Kidney Disease

Ananda Staats Pires[1,2#], Shabarni Gupta[3#], Sean A Barton[3], Roshana Vander Wall[3], Vanessa Tan[1], Benjamin Heng[1], Jacqueline K Phillips[3] and Gilles J Guillemin[1]

[1]Neuroinflammation Group, Macquarie Medical School, Centre for Motor Neuron Disease Research, Faculty of Medicine, Health and Human Sciences, Macquarie University, Sydney, NSW, Australia. [2]Laboratório de Bioenergética e Estresse Oxidativo, Departamento de Bioquímica, Centro de Ciências Biológicas, Universidade Federal de Santa Catarina, Florianópolis, Brasil. [3]Autonomic and Sensory Neuroscience Group, Macquarie Medical School, Faculty of Medicine, Health and Human Sciences, Macquarie University, Sydney, NSW, Australia.

ABSTRACT: Autosomal recessive polycystic kidney disease (ARPKD) is an early onset genetic disorder characterized by numerous renal cysts resulting in end stage renal disease. Our study aimed to determine if metabolic reprogramming and tryptophan (Trp) metabolism via the kynurenine pathway (KP) is a critical dysregulated pathway in PKD. Using the Lewis polycystic kidney (LPK) rat model of PKD and Lewis controls, we profiled temporal trends for KP metabolites in plasma, urine, and kidney tissues from 6- and 12-week-old mixed sex animals using liquid and gas chromatography, minimum $n = 5$ per cohort. A greater kynurenine (KYN) concentration was observed in LPK kidney and plasma of 12-week rats compared to age matched Lewis controls ($P \leqslant .05$). LPK kidneys also showed an age effect ($P \leqslant .05$) with KYN being greater in 12-week versus 6-week LPK. The metabolites xanthurenic acid (XA), 3-hydroxykynurenine (3-HK), and 3-hydroxyanthranilic acid (3-HAA) were significantly greater in the plasma of 12-week LPK rats compared to age matched Lewis controls ($P \leqslant .05$). Plasma XA and 3-HK also showed an age effect ($P \leqslant .05$) being greater in 12-week versus 6-week LPK. We further describe a decrease in Trp levels in LPK plasma and kidney (strain effect $P \leqslant .05$). There were no differences in KP metabolites in urine between cohorts. Using the ratio of product and substrates in the KP, a significant age-strain effect ($P \leqslant .05$) was observed in the activity of the KYN/Trp ratio (tryptophan-2,3-dioxygenase [TDO] or indoleamine-2,3-dioxygenase [IDO] activity), kynurenine 3-monooxygenase (KMO), KAT A (kynurenine aminotransferase A), KAT B, total KAT, total KYNU (kynureninase), KYNU A, KYNU B, and total KYNU within LPK kidneys, supporting an activated KP. Confirmation of the activation of these enzymes will require verification through orthogonal techniques. In conclusion, we have demonstrated an up-regulation of the KP in alignment with progression of renal impairment in the LPK rat model, suggesting that KP activation may be a critical contributor to the pathobiology of PKD.

KEYWORDS: Kynurenine pathway, tryptophan, chronic kidney disease, polycystic kidney disease, nephronophthisis

Introduction

Polycystic kidney disease (PKD) is a genetically heterogenous class of kidney disease with diverse clinical manifestations, commonly characterized by progressive development of renal cysts.[1,2] These diseases manifest as early as in utero or remain dormant until their presentation in adulthood, ultimately resulting in renal failure.[3] Broadly, the spectrum of symptoms of PKD includes hypertension, polydipsia, polyuria, proteinuria, abdominal/flank pain, nephrolithiasis, and electrolyte imbalance, alongside a heterogenous combination of additional presentations depending on if the disease is inherited in an autosomal dominant (adult onset) or autosomal recessive (in-utero/childhood onset) fashion.[1] Alternatively, it is a part of a syndromic presentation resulting from ciliopathies (diseases of cilia).[4,5] As renal function diminishes with increase in number/size of cysts, accumulation of uremic toxins further deteriorates the health of affected individuals.[6] Disease management strategies are primarily palliative, with no cure or course of reversal. Tolvaptan, a vasopressin receptor 2 antagonist has recently been approved by the US FDA as a drug to slow cystogenesis, thereby retarding disease progression.[7,8] However, due to notable side effects it is recommended to be prescribed in short courses and to individuals with rapid cystic progression.[1] For PKD patients, once end stage renal disease (ESRD) is reached, a regime of highly invasive renal replacement therapy (RRT) including dialysis and renal transplants remains the only therapeutic modalities.

#Co-first authors

PKD is classified as autosomal dominant PKD (ADPKD), mainly caused by mutations in *PKD1* and *PKD2*[1] and autosomal recessive PKD (ARPKD), predominantly caused by mutations in *PKHD1*.[2,3] Nephronophthisis (NPHP) is another form of cystic kidney disease. It can present as isolated renal pathology or as part of a syndromic condition such as Bardet–Biedl, Joubert, and Meckel syndrome[2,9] and is the most common genetic cause of renal failure in children.[3] There are over 21 genes known to cause NPHP.[10] Mutations in the *NIMA related kinase 8 (Nek8)* gene is causative of NPHP9. In humans, *Nek8* mutations in loci H425Y, A497P, and L330F have been reported clinically[11] and 2 prominent animal models harboring Nek8 mutations are the juvenile cystic kidney (*jck*) mouse harboring a G448V mutation[12] and the Lewis Polycystic Kidney (LPK) rat model with a mutation at the R650C locus of Nek8.[13,14]

Although PKD is a genetic disease, studies indicate that aberrations in cellular metabolism is an integral component of disease pathogenesis.[15] This includes disturbances in central metabolic pathways such as glucose metabolism, lipid metabolism and OXPHOS pathways.[16,17] While there are several studies focused on the metabolic aberrations of ADPKD,[18-23] very few profile ARPKD. Metabolic profiling of the ARPKD *cpk* mouse model, harboring a mutation in the *Cys1* gene, revealed glutamine dependent overproduction of oncometabolite 2-hydroxyglutarate.[24] Studies on models harboring the *NPHP9/Nek8* mutation include the seminal metabolomic study by Taylor et al who reported a global, temporal, metabolomic profile of the urine from the *jck* mouse model.[25] Two other studies by Abbiss et al incorporated a global metabolomic profile of the urine, kidney, and liver tissue of the LPK rat.[26,27] In each of these rodent models, tryptophan (Trp) levels were found to be dysregulated.

Trp is an essential amino acid and is the least available of all proteinogenic amino acids, so its availability is an important factor in the control of protein biosynthesis.[28] Apart from its incorporation into proteins, Trp can be metabolized: (i) through the serotonin pathway[29]; (ii) through the glutarate pathway[30]; and mainly (iii) metabolized by enzymes though the kynurenine pathway (KP),[31] accounting for ~95% of Trp degradation. The rate-limiting step in Trp metabolism through the KP is the enzymatic conversion of Trp to N-formylkynurenine by indoleamine-2,3-dioxygenase (IDO)1, IDO2 and tryptophan-2,3-dioxygenase (TDO), which vary in distribution, substrate affinity, and inducing factors.[32] Subsequently, N-formylkynurenine is transformed into kynurenine (KYN), the central intermediate of the KP, by formamidase. KYN can be metabolized to a number of metabolites depending on the extent of the KP enzymes expression and activity in a particular tissue or cell type. KYN may be metabolized into anthranilic acid (AA) or kynurenic acid (KYNA) by kynureninase (KYNU) and kynurenine aminotransferases (KATs I, II, and III), respectively. Additionally, kynurenine 3-monooxygenase (KMO) may transform KYN into 3-hydroxykynurenine (3-HK) to produce 3-hydroxyanthranilic acid (3-HAA) by KYNU. 3-HAA in turn, forms picolinic acid (PIC), quinolinic acid (QUIN) and nicotinamide adenine dinucleotide (NAD+) though the action of additional enzymes. 3-HK can also be metabolized by KATs into xanthurenic acid (XA)[33,34] (Figure 1).

The metabolization of KYN by these enzymes can have fundamental consequences on cellular function and survival. The KP metabolites include compounds that have been identified as neurotransmitter agonists or antagonists,[35,36] neurotoxins,[37] immunomodulators,[38] and pro- and/or antioxidants.[39] The main route of elimination of KYN and its metabolites is renal excretion.[40] The kidney is able to uptake KYN and 3-HK from the blood, which are metabolized and excreted in the form of KYNA and XA, respectively.[41] Thus, the impairment of kidney function is likely to be associated with the accumulation of KP metabolites. Indeed, abnormalities in Trp metabolism, such as a decrease in serum Trp concentration with increased levels of KYN have been reported in humans and rats with chronic renal insufficiency.[42-48] Therefore, the measurement of KP metabolites in body fluids may be a sensitive indicator of kidney disease severity and/or progression. Furthermore, most of the metabolites of KP show diverse biological activity. The temporal changes in concentration of these metabolites through the course of renal disease and their impact are not explored. Existing evidence of aberrations in Trp metabolism in kidney disease sets the premise for a targeted investigation of this pathway in a rodent model of PKD. In the present study we evaluated Trp metabolism via the KP by studying plasma, kidney tissues and urine using liquid and gas chromatography techniques and quantifying KP metabolites using the LPK rodent model.

Materials and Methods

Animals

Experiments were conducted with approval from Macquarie University Animal Ethics Committee and in adherence to the Australian Code of Practice for the Care and Use of Animals for Scientific Purposes. Female and male Lewis and LPK rats (Animal Resources Centre, Perth, Australia) were acclimatized to their new environment upon arrival and group-housed (group of 4 rats per cage) in a 12 hours light followed by 12 hours dark cycle at the Central Animal Facility, Macquarie University. The animals had access to standard laboratory rat chow and water ad libitum.

Sample collection

Biospecimens used in this study were obtained from archival samples of LPK and Lewis animals aged 6 and 12 weeks (Supplemental Table S1). These time points were selected
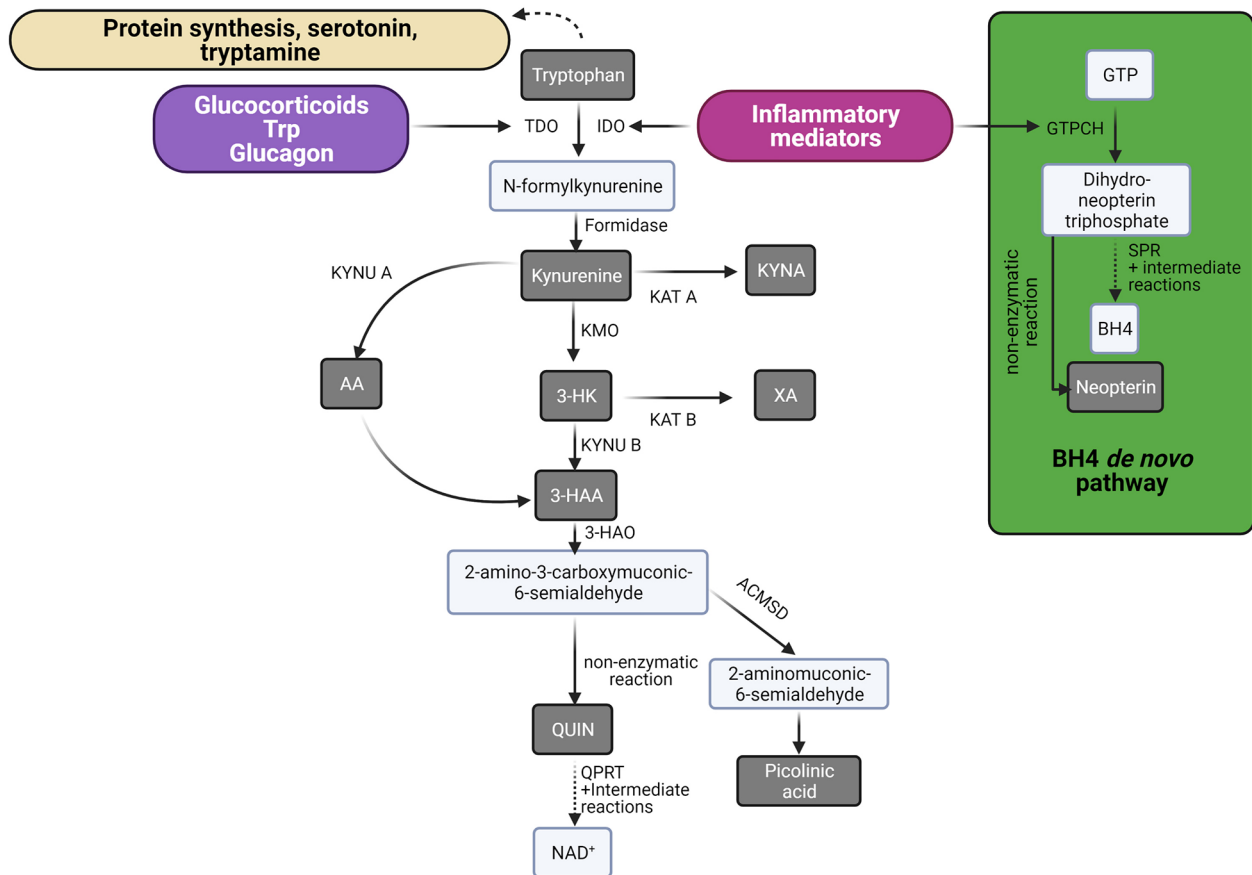
Figure 1. The kynurenine pathway. This schematic illustrates tryptophan (Trp) metabolism though the kynurenine pathway. Tryptophan 2,3-dioxygenase (TDO), one of the rate-limiting enzymes of the kynurenine pathway is up-regulated by elevated glucocorticoids, glucagon and Trp. The kynurenine pathway is also activated under inflammatory conditions. Inflammatory mediators also activate the tetrahydrobiopterin (BH4) pathway. Indoleamine 2,3-dioxygenase (IDO) and guanosine triphosphate cyclohydrolase I (GTPCH), the rate-limiting enzymes of the kynurenine and BH4 pathways, respectively are activated in the presence of inflammatory mediators. Activation of the BH4 pathway results in the accumulation of the metabolite neopterin, an established sensitive biomarker for inflammatory activation and a surrogate for IDO activation. Once activated, the kynurenine pathway transforms the amino acid Trp into a series of intermediates through specific enzymes catalyzing each reaction in various cells/tissues. The metabolites that were measured in the present study are highlighted in gray (Adapted and redrawn from Staats Pires et al[50]).
Abbreviations: 3-HAA, 3-hydroxyanthranilic acid; 3-HAO, 3-hydroxyanthranilic acid 3,4-dioxygenase; 3-HK, 3-hydroxykynurenine;AA, anthranilic acid; ACMSD, 2-amino-3-carboxymuconate-6-semialdehyde decarboxylase; GTP, guanosine triphosphate; KATs, kynurenine aminotransferases; KMO, kynurenine 3-monooxygenase; KYNA, kynurenic acid; KYNU, kynureninase; NAD+, nicotinamide adenine dinucleotide; QPRT, quinolinate phosphoribosyltransferase; QUIN, quinolinic acid; SPR, sepiapterina reductase.

being ages where animals have early and established renal disease, respectively, but have not yet progressed to end stage renal failure.[13] A minimum of $n = 5$ animals was used for each biospecimen. While attempts were made to sex match this was not achieved in all cases due to archival tissue sample availability.

For urine, animals were placed in a metabolic cage for ~4 hours for sample collection. Urine was then spun and stored at −80°C until further use. Plasma and kidney tissue samples were collected immediately after euthanasia, which was performed using either sodium pentobarbitone (Thiobarb, Jurox, Rutherford, Australia; intraperitoneal injection (100 mg/kg)) or exposure to isoflurane gas (5% in 100% O_2) until breathing ceased. Blood was collected via cardiac puncture into K_2-EDTA tubes, then centrifuged, plasma separated, collected and stored at −80°C until further use. The left kidney was snap-frozen and stored at −80°C.

Analytical biochemistry to monitor kidney function in animals

Plasma urea, creatinine, and the ratio of blood urea nitrogen (BUN) to creatinine (BUN/Crea) were determined using an IDEXX VetTest® analyzer (IDEXX, NSW Australia) to establish disease condition in the animals. Urinary creatinine and urine protein creatinine ratio (UPC) was also measured using IDEXX kits to monitor decline in renal function, however a more sensitive colorimetric creatinine assay was used to normalize metabolite concentrations in urine samples (elaborated in subsequent sections). Creatinine clearance in plasma was calculated using the formula:

$$\text{Creatinine clearance} \left(\text{mL min}^{-1} \right) = \frac{\text{urinary creatinine} \left(\mu\text{mol}^{-1} \right) \times \text{urine rate} \left(\text{mL min}^{-1} \right)}{\text{plasma creatinine} \left(\mu\text{mol}^{-1} \right)}$$

Protein determination

The protein content in the kidney samples were determined by the Pierce bicinchoninic acid (BCA) protein assay, using a commercial kit (Thermo Scientific Pierce BCA Protein Assay Kit, Rockford, USA) and following the manufacturer's technical recommendations. The protein content estimated in this assay was used to normalize the KP metabolites in kidney samples.

Creatinine determination for metabolite normalization

The urinary creatinine concentrations were determined by colorimetric assay using a commercial kit (Abcam, Cambridge, MA) and following the manufacturer's technical recommendations. The creatinine estimated in this assay was used to normalize the KP metabolites in urine samples.

Kidney sample processing

Snap frozen sections of kidney were weighed and homogenized with addition of sodium acetate (100 mM, pH 4.65) using a Precelly 24-dual homogenizer (Bertin Instruments, Montignyle-Bretonneux, France) in accordance with the manufacturer instructions. Supernatants were transferred to a fresh microtube, and the samples were deproteinised by adding 1 vol. of 10% trichloroacetic acid containing 6.5 mM dithioerythritol. Afterward, samples were centrifuged at $12\,000\times g$ at 4°C for 20 minutes and the supernatant concentrated using a Savant SpeedVacH Concentrator (Thermo Scientific, MA, USA). Dried samples were resuspended in 10% trichloroacetic acid and filtered through a 0.20 μm PTFE syringe filter (Merck-Millipore, CA, USA). Samples were then transferred to high performance liquid chromatography **(**HPLC) vials for analysis.

Plasma and urine sample processing for KP analysis

Plasma and urine samples were deproteinised by adding 1 vol. of 10% trichloroacetic acid containing 6.5 mM dithioerythritol. Afterward, samples were centrifuged at $12\,000\times g$ at 4°C for 15 minutes and filtered through a 0.20 μm PTFE syringe filter (Merck-Millipore, CA, USA). Supernatants were transferred to HPLC vials for analysis. The urine samples were further diluted in ultrapure water prior the HPLC analysis when necessary.

Sample derivatization

Deproteinised samples and deuterated internal standards were dried under vacuum and derivatized with trifluoroacetic anhydride for 10 minutes at 60°C followed by 1,1,1,3,3,3-hexafluoroisopropanol for extra 10 minutes at 60°C. Fluorinated

esters were then extracted into toluene and washed with 5% sodium bicarbonate. The upper organic layer was collected and washed with 1 mL MilliQ water, and dried using sodium sulfate packed pipette tips. Samples were then transferred to gas chromatography/mass spectrometry (GC/MS) vials for analysis.

Samples' concentration of XA, Trp, KYN, 3-HK, 3-HAA, and AA were determined by HPLC and quantified using a sequential diode-array UV and fluorescence detection as previously described.[49] The HPLC analysis was carried out in an uHPLC system (Agilent 1290 Infinity, CA, USA) by using an Agilent ZORBAX Rapid Resolution High Definition C18, reversed phase column (2.1×150 mm, 1.8 μm, Agilent Technologies, CA, USA). The temperature of the column compartment was set at 38°C. Injection volume was 20 μL and the autosampler tray temperature was set at 4°C to prevent sample degradation. The flow rate was set at 0.75 mL/min with an isocratic elution of 100% of 100 mM sodium acetate, pH 4.65. The identification and quantification of XA, KYN, and 3-HK were performed by a UV detector (G4212A, Agilent, CA, USA) with absorbance at 250 nm and a reference signal at 350 nm for XA: and with absorbance at 365 nm and a reference signal off for KYN and 3-HK. The identification and quantification of Trp, 3-HAA, and AA were performed by a fluorescence detector (G1321B xenon flash lamp, Agilent, CA, USA) with emission wavelength of 438 nm and an excitation wavelength of 280 nm for Trp and 320 nm for 3-HAA and AA. The results were calculated by interpolation using a 6-point calibration curve and expressed as μmol/L or nmol/L for plasma, as μmol/mmol creatinine or nmol/mmol creatinine for urine and as μmol/g or nmol/g protein for kidney samples.

Neopterin (NEO) concentrations in samples were determined as previously described by Staats Pires et al.[50] The same HPLC system and column described previously were used with a mobile phase of 100% of 15 mM potassium phosphate buffer, pH 6.4. The flow rate was set at 0.7 mL/min with an isocratic elution. The identification of NEO was performed by a fluorescence detector (G1321B xenon flash lamp, Agilent, CA, USA) with emission wavelength of 438 nm and an excitation wavelength of 355 nm. The results were calculated by interpolation using 6-point calibration curve. Levels of NEO were calculated and expressed as nmol/L for plasma, as nmol/mmol creatinine for urine and as nmol/g protein for kidney samples.

KYNA concentrations in samples were determined by HPLC (Agilent 1260 Infinity, Agilent, CA, USA) and an Agilent ZORBAX Rapid Resolution High Definition C18, reversed phase (4.6×100 mm, 3.5 μm, Agilent Technologies, CA, USA). Mobile phase consisted of 95% of 50 mM sodium acetate and 50 mM zinc acetate, pH 5.2 and 5% HPLC grade acetonitrile. The flow rate was set at 1.00 mL/min with an isocratic elution. The identification of KYNA was performed by a

Table 1. Analytical biochemical profiles of parameters determining kidney function in 12-week Lewis and LPK animals.

PLASMA			
	Lewis ($X \pm$ SD; $n=6$)	LPK ($X \pm$ SD; $n=8$)	Adj. *P*-value
Plasma creatinine μmol/L*	15.67 ± 2.94	56.25 ± 20.47	.0005
Plasma urea (mmol/L)*	6.817 ± 1.15	20.53 ± 5.71	<.0001
BUN/Crea*	32.67 ± 9.20	65.17 ± 8.56	<.0001
Creatine clearance rate* (mL/min)	3.545 ± 1.06	1.115 ± 0.93	.0007
URINE			
	Lewis ($X \pm$ SD; $n=6$)	LPK ($X \pm$ SD; $n=5$)	Adj. *P*-value
Urine creatinine (g/L)*	5.42 ± 1.65	1.10 ± 0.21	.0003
UPC*	0.16 ± 0.07	7.81 ± 4.18	.0014

All data are presented as mean ± standard deviation ($X \pm$ SD). * indicates significant (*P*-value ≤ .05) using unpaired Student's *t*-test.

fluorescence detector (G1321B xenon flash lamp, Agilent, CA, USA) with emission wavelength of 388 nm and an excitation wavelength of 344 nm. The results were calculated by interpolation using a 6-point calibration curve. Levels of KYNA were calculated and expressed as nmol/L for plasma, as μmol/mmol creatinine for urine and as nmol/g protein for kidney samples.

Metabolites quantification by GC/MS

QUIN and PIC concentrations in samples were determined using an Agilent 7890 gas chromatograph coupled with an Agilent 5975 mass spectrometer following a protocol previously described.[49] Briefly, samples were injected under a splitless mode onto a HP-5MS GC capillary column (Agilent, CA, USA) and the analysis was carried out with the MS operating in negative chemical ionization mode. Selected ions (m/z 273 for PIC, m/z 277 for 4-PIC, m/z 467 for QUIN, and m/z 470 for d3-QUIN) were simultaneously monitored. GC oven settings were as follows: oven temperature was held at 75°C for 3 minutes and then ramped to 290°C at a rate of 25°C/min and held at 290°C for 4 minutes for a total run time of 15.6 minutes. Quantification was achieved through normalization with respect to the internal standards and interpolation using 6-point calibration curves for each metabolite. Levels were calculated and expressed as nmol/L for plasma, as nmol/mmol creatinine for urine and as nmol/g protein for kidney samples.

Statistical Analysis

Statistical significance of kidney function parameters such as plasma urea, plasma creatinine, BUN/Crea, creatinine clearance rate, urinary creatinine and UPC was evaluated using (Prism 8.0.2, GraphPad Software Inc.). Concentration of KP metabolites in the studied cohorts were subjected to a preliminary analysis (IBM Statistical Package for the Social Sciences [SPSS], v25) to identify age, strain and sex effects using a univariate general linear model. No sex effect was identified for any of the variables and subsequent analysis was undertaken with age and strain as the identified fixed factors (Two-way ANOVA). Levene's Test of Equality of Variances was used to test for sample variance (equal variances assumed if median *P* > .05). Multiple comparisons of age-strain groups were performed using Bonferroni post-hoc analysis (when equal variances assumed), or a Dunnett's T3 test (when equal variances not assumed). An adjusted *P* ≤ .05 was considered significant for all analyzes.

Results

Plasma urea and creatinine concentrations in Lewis and LPK cohorts

The analytical biochemical parameters plasma urea, creatinine, BUN/Crea ratio, urinary creatinine, UPC and creatinine clearance rate for Lewis and LPK rats at 12 weeks were evaluated to establish the presence of renal disease in the LPK model.

Table 1 shows significant increase in plasma creatinine, urea, BUN/Crea ratio and UPC and decrease in urine creatinine and creatinine clearance rate in LPK as compared to Lewis rats.

Temporal profile of the KP metabolite levels in plasma of LPK and Lewis groups

Figure 2 shows the temporal differences in KP metabolites in plasma from LPK and Lewis rats from 6 to 12 weeks of age. There was a significant age-strain effect on the levels of KYN, XA, 3-HK, and 3-HAA. In the case of XA, 3-HK, 3-HAA these effects were driven by the significantly high levels of metabolites in the 12-week LPK in comparison to all other groups. Similarly,
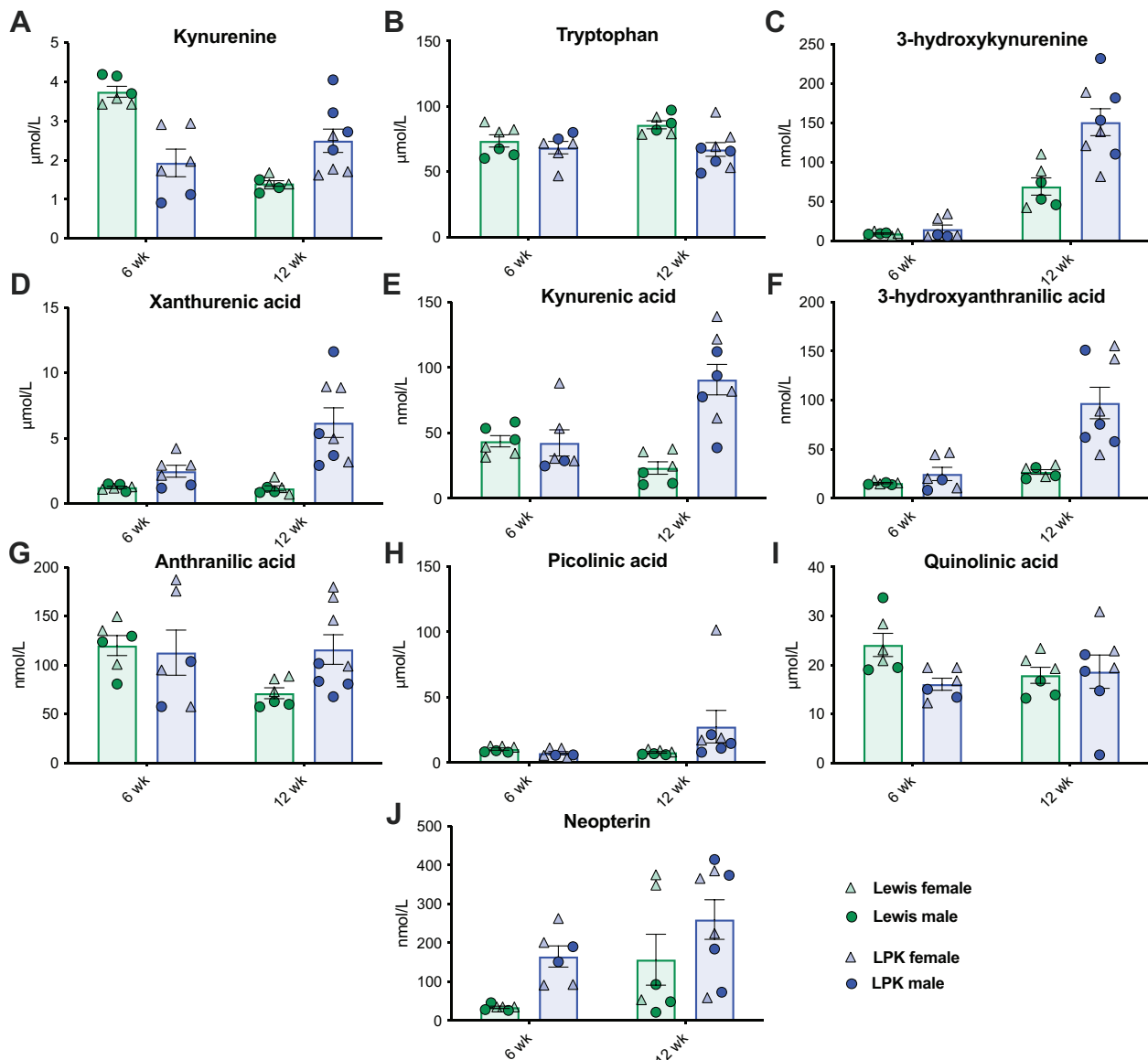
Figure 2. Levels of kynurenine pathway metabolites and neopterin in the plasma of LPK and Lewis control groups: plasma levels of (A) kynurenine, (B) tryptophan, (C) 3-hydroxykynurenine, (D) xanthurenic acid, (E) kynurenic acid, (F) 3-hydroxyanthranilic acid, (G) anthranilic acid, (H) picolinic acid, (I) quinolinic acid, and (J) neopterin in LPK rats and Lewis control rats. All data are presented as mean ± SEM. Green represents the Lewis rats, while blue represents LPK rats. Each dot represents a single male rat, and each triangle represents a single female rat.
Abbreviation: LPK: lewis polycystic kidney; wk: weeks.

the 6-week Lewis animals showed significantly higher KYN in comparison to all other groups. Trp and KYNA showed only a significant strain effect, with lower Trp, (FC = 0.85, *P*-value = .015) and higher KYNA levels (FC = 2.1, *P*-value = .003) in LPK when compared to Lewis. For circulating levels of NEO there was a statistically significantly age (higher in 12-week-old animals; FC = 2.16, *P*-value = .04) and strain (higher in LPK animals; FC = 2.29, *P*-value = .02) effect, however a combined age-strain effect was not evident after performing post-hoc analysis. Complete KP metabolite plasma profile and statistical analysis from multiplex comparisons can be found in the supplemental information (Supplementary Table S2).

Temporal profile of the KP metabolite levels within kidney tissues of LPK and Lewis groups

Figure 3 shows the levels of Trp and KP metabolites in the kidney of the LPK and Lewis rats at 6 and 12 weeks of age. KYN levels showed a significant age and strain effect. XA (FC = 28.31, *P*-value = .01), KYNA (FC = 23.54, *P*-value = .01), 3-HAA (FC = 19.92, *P*-value = .01), AA (FC = 13.70, *P*-value = .01), and QUIN (FC = 12.05, *P*-value = .01) demonstrated a significant strain effect only, being significantly higher in the LPK animals when compared to Lewis. Trp concentration in kidneys showed a significant age effect and strain effect, with Trp levels lower in 12-week-old and LPK animals, respectively.
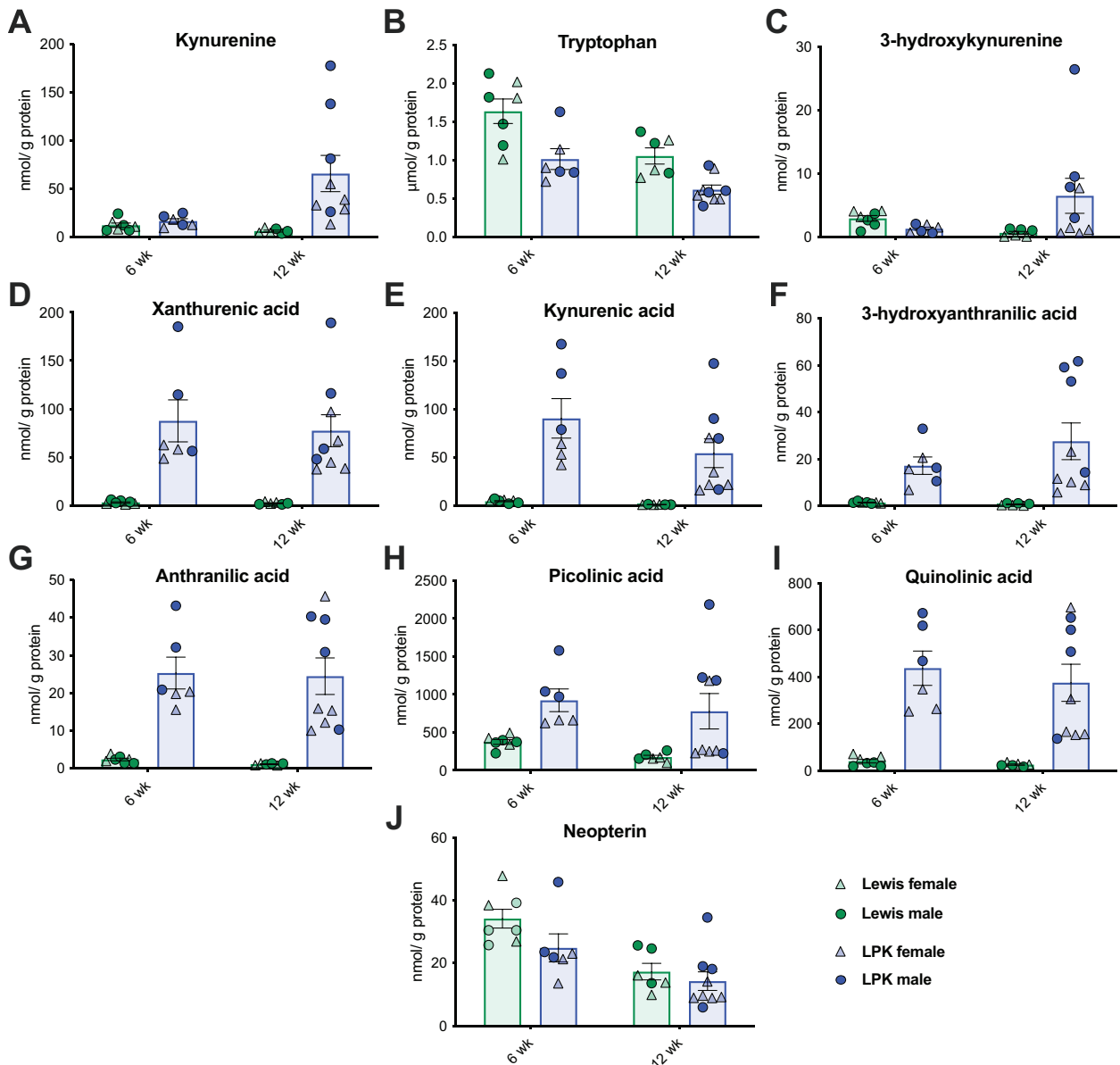
Figure 3. Levels of kynurenine pathway metabolites and neopterin in the kidney of LPK and Lewis control groups: kidney levels of (A) kynurenine, (B) tryptophan, (C) 3-hydroxykynurenine, (D) xanthurenic acid, (E) kynurenic acid, (F) 3-hydroxyanthranilic acid, (G) anthranilic acid, (H) picolinic acid, (I) quinolinic acid, and (J) neopterin in LPK rats and Lewis control rats. All data are presented as mean ± SEM. Green represents the Lewis rats, while blue represents LPK rats. Each dot represents a single male rat, and each triangle represents a single female rat.
Abbreviation: LPK: lewis polycystic kidney; wk: weeks.

However, a combined age-strain effect was not evident after performing post-hoc analysis. The complete kidney tissue profile of KP metabolites and statistical results from various comparisons can be found in the supplemental information (Supplemental Table S3).

Temporal profile of the KP metabolite levels in urine of LPK and Lewis groups

An analysis of levels of KP metabolites in the urine identified an age effect for KYN but no strain effect (Figure 4), with levels being lower in the 12-week (FC = 0.45, *P*-value = .01) in

comparison to 6-week-old animals. While 3-HAA and NEO showed a significant age effect and strain effect, a combined age-strain effect was not evident in the post-hoc analysis. The full urinary KP metabolite profile with statistical analysis can be found in the supplemental information (Supplemental Table S4).

KP enzyme activity in plasma, kidney tissue, and urine of LPK and Lewis groups

An indirect analysis of the activity of the other downstream KP enzymes in plasma, kidney tissue and urine were estimated by the product/substrate ratios. Table 2 lists the significant
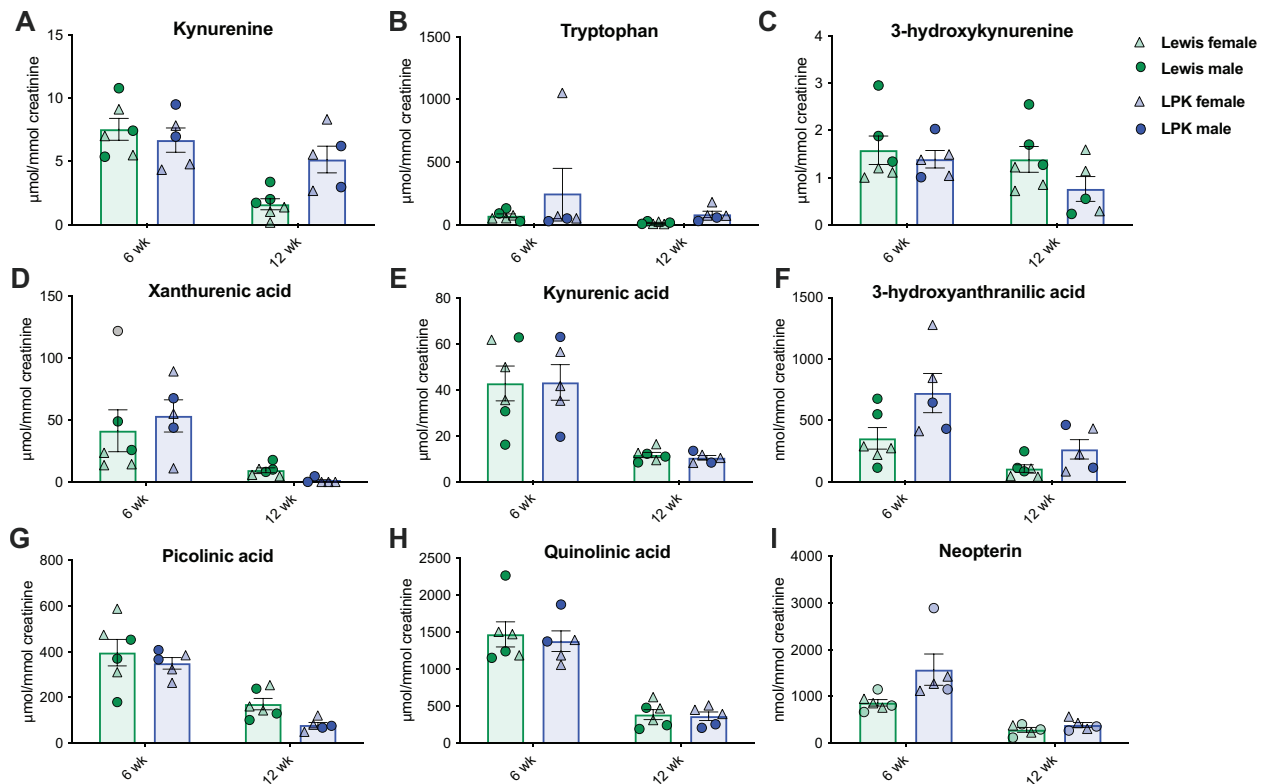
Figure 4. Levels of kynurenine pathway metabolites and neopterin in the urine of LPK and Lewis control groups: urine levels of (A) kynurenine, (B) tryptophan, (C) 3-hydroxykynurenine, (D) xanthurenic acid, (E) kynurenic acid, (F) 3-hydroxyanthranilic acid, (G) picolinic acid, (H) quinolinic acid, and (I) neopterin in LPK rats and Lewis control rats. All data are presented as mean ± SEM. Green represents the Lewis rats, while blue represents LPK rats. Each dot represents a single male rat, and each triangle represents a single female rat.
Abbreviation: LPK: lewis polycystic kidney; wk: weeks.

changes in KP enzyme activities across these biospecimens (noting that none of the enzymes were found to have a significant change in urine). A significant age-strain effect driven by the significantly elevated levels of plasma 3-HAA/AA ratio in 12-week LPK animals was observed in comparison to all other groups.

A similar significant age-strain effect was also seen in kidney KYN/Trp ratio (indicating TDO or IDO activity), KMO, KAT A, KAT B, total KAT, KYNU A, KYNU B, and total KYNU. Post-hoc analysis indicated that the changes in IDO/TDO were driven by elevated KYN/Trp ratio in the 12-week LPK animals in comparison to all other groups where as KMO was driven by elevated 3-HK/KYN in 12-week Lewis animals in comparison to all other groups. Indirect estimated enzyme activity of KAT A, KAT B, total KAT, KYNU A, KYNU B, and total KYNU in kidneys were all found to be significantly high in the 6-week LPK animals in comparison to all other groups, explaining the observed age-strain effect.

The complete experimental data set is provided in the Supplementary Data. Detailed individual animal data for each cohort is provided in **Supplementary Data SD1**. The extended values of urea and creatinine values across the various samples can be found in **Supplementary Data SD2**.

The extended values of normalized data for KP metabolites in plasma and statistical analysis of KP metabolites in plasma can be found in **Supplementary Data SD3** and **SD4**, respectively. The extended values of normalized data for KP metabolites in kidney and statistical analysis of KP metabolites in kidney can be found in **Supplementary Data SD3** and **SD4**, respectively. The extended values of normalized data for KP metabolites in urine and statistical analysis of KP metabolites in urine can be found in **Supplementary Data SD5** and **SD6**, respectively.

Discussion

There are numerous studies associating disturbances in Trp metabolism and the accumulation of KP metabolites to neurological disorders, impaired lipid metabolism and uremia, as well as vascular endothelial dysfunction leading to atherosclerosis and cardiovascular incidents.[51] While the effects of KP metabolites on renal function are unexplored, the results observed in our study provide novel insights on trends of KP metabolites and its possible implication in renal function contributing to cystic disease progression. The present study was performed on the LPK rat model to assess changes in KP metabolism governing Trp metabolism. Plasma concentration of the uremic toxins

Table 2. Temporal changes in KP enzyme activity# in plasma and kidney from 6- to 12-week Lewis and LPK animals.

PLASMA										
NO.	ENZYME#	WEEK 6				WEEK 12				2-WAY ANOVA	
		LEWIS (*N*=6)		LPK (*N*=6)		LEWIS (*N*=6)		LPK (*N*=8)		ADJ. *P*-VALUE (AGE)	ADJ. *P*-VALUE (STRAIN)
		MEAN	SD	MEAN	SD	MEAN	SD	MEAN	SD		
1	3-HAA/AA ratio*	0.14	0.04	0.22	0.09	0.39	0.07	0.86	0.33	.01	.01
2	TDO or IDO (KYN/Trp ratio [×100])	5.25	1.2	2.95	1.39	1.65	0.27	3.94	1.64	.01	.49
3	KMO (3-HK/KYN ratio [×100])	0.34	0.11	0.93	0.27	1.29	0.57	2.73	1.21	.01	.01
4	KAT A (KYNA/KYN ratio [×100])	1.17	0.24	2.25	0.71	1.64	0.74	4.01	1.89	.02	.01
5	KAT B (XA/3-HK ratio [×100])	10486.55	2912.58	16932.13	11738.8	8531.68	7406.52	9403.6	5989.33	.22	.29
6	total KAT (KAT *A* + KAT B)	10487.71	2912.8	16934.38	11738.41	8533.32	7406.74	9407.15	5990.53	.22	.29
7	KYNU A (AA/KYN ratio [×100])	3.23	0.76	6.02	1.97	5.08	0.78	5.36	3.01	.46	.01
8	KYNU B (3-HAA/3-HK ratio [×100])	135.6	52.7	134.68	37.87	177.86	75.3	153.14	107.95	.22	.78
9	total KYNU (KYNU *A* + KYNU B)	138.82	52.22	140.7	38.49	182.94	75.88	158.04	109.43	.22	.83
KIDNEY										
NO.	ENZYME#	WEEK 6				WEEK 12				2-WAY ANOVA	
		LEWIS (*N*=7)		LPK (*N*=6)		LEWIS (*N*=6)		LPK (*N*=9)		ADJ. *P*-VALUE (AGE)	ADJ. *P*-VALUE (STRAIN)
		MEAN	SD	MEAN	SD	MEAN	SD	MEAN	SD		
1	3-HAA/AA ratio	0.7	0.25	0.71	0.35	0.65	0.32	1.05	0.49	.04	.01
2	TDO or IDO (KYN/Trp ratio [×100])*	0.76	0.42	1.67	0.57	0.6	0.33	10.06	6.95	.01	.01
3	KMO (3-HK/KYN ratio [×100])*	4.01	2.58	0.79	0.8	23.23	19.7	7.65	3.66	.01	.01
4	KAT A (KYNA/KYN ratio [×100])*	42.52	19.03	536.43	157.84	19.49	4.43	90.28	33.75	.01	.01
5	KAT B (XA/3-HK ratio [×100])*	904.62	508.11	152127	144804.5	282.74	142.84	2452.13	1240.33	.01	.01
6	total KAT (KAT *A* + KAT B)*	947.14	511.7	152663.4	144895.1	302.22	143.01	2542.4	1259.91	.01	.01

(Continued)

Table 2. (Continued)

NO.	ENZYME#	WEEK 6				WEEK 12				2-WAY ANOVA	
		LEWIS (N=7)		LPK (N=6)		LEWIS (N=6)		LPK (N=9)		ADJ. P-VALUE (AGE)	ADJ. P-VALUE (STRAIN)
		MEAN	SD	MEAN	SD	MEAN	SD	MEAN	SD		
7	KYNU A (AA/KYN ratio [×100])*	23.18	12.54	157.74	36.47	20.96	5.99	46.7	20.64	.01	.01
8	KYNU B (3-HAA/3-HK ratio [×100])*	427.18	161.38	25181.33	15472.86	159.56	163.36	653.45	329.49	.01	.01
9	total KYNU (KYNU A + KYNU B)*	450.36	169.65	25339.06	15483.44	180.51	166.73	700.14	325.05	.01	.01

#Activity of the other downstream KP enzymes in the plasma and kidney, estimated indirectly though the ratio of product/substrate. Activities of these enzymes were not significant in the urine. * indicates significant (P-value ⩽ .05) age-strain interaction effect in post-hoc analysis.
Abbreviations: 3-HAA, 3-hydroxyanthranilic acid; 3-HK, 3-hydroxykynurenine; AA: anthranilic acid; IDO, indoleamine-2,3-dioxygenase; KAT: kynurenine aminotransferase; KMO: kynurenine 3-monooxygenase; KYN, kynurenine; KYNA, kynurenine acid; KYNU: kynureninase; LPK: Lewis polycystic kidney; TDO, tryptophan-2,3-dioxygenase; Trp, Tryptophan; XA: xanthurenic acid.

urea and creatinine, determination of creatinine clearance, along with urinary creatinine levels and urine protein creatine ratio levels were used to assess renal function in LPK animals relative to the control Lewis strain. Renal function was significantly impaired, which is in accordance with our previous studies that establish a clear progression of disease over the ages of 6-12 weeks.[13] Trp metabolites generated via the KP have been profiled in chronic kidney diseases, with dysregulation of Trp metabolism reported to be causative of fatigue, proteinuria, and uremic symptoms present in these patients.[52-54] The metabolites of the KP, individually, have however, never been profiled in subjects with cystic kidney disease, to the best of our knowledge. Aberrations in Trp metabolism have been shown previously using global metabolomics approaches in PKD models[24,25] including the LPK.[26,27] Our study extends this work by dissecting and profiling the metabolites of the KP in cystic disease phenotypes using a targeted metabolomic approach.

Major findings of the present study are *i)* a simultaneous decrease in Trp level alongside increased KP metabolites in 12-week-old LPK kidneys, and *ii)* a temporal increase in KP metabolites in LPK plasma.

i. Regarding the increase of KP metabolites as observed across temporal profiles of LPK biospecimens, this suggests an activation of TDO or IDO triggering Trp metabolism via this pathway. This is further supported by our observed increase in KYN to Trp ratio, an index of TDO/IDO activity, in both 12-week plasma and kidney tissue from LPK rats. Since TDO and IDO are regulated by different mechanisms,[55] increased plasma and kidney levels of KP metabolites might result from activation of either enzyme. TDO expression levels are regulated mostly by systemic levels of Trp, glucagon and

corticosteroids,[56] whereas the expression and activity of IDO are induced mainly by the pro-inflammatory cytokines.[57] Under inflammatory conditions, the rate-limiting enzyme of tetrahydrobiopterin biosynthesis, guanosine triphosphate cyclohydrolase I, is upregulated while downstream enzymes of this pathway remain just slightly increased. This metabolic blockage results in the accumulation of neopterin, an established sensitive biomarker for inflammatory activation.[50] Inflammatory factors, and not glucagon/stress hormones, concurrently with IDO stimulate the rate-limiting enzyme of pteridines pathway with consequent formation of neopterin (Fig. 1). Assessment of neopterin levels thereby help in differentiating between TDO and IDO-induced elevation of KYN. Without assessment of neopterin levels, it is difficult to attribute the observed differences in KYN/Trp ratio to activation of TDO or IDO.[58] In the present study, the neopterin levels were not significantly different between the groups analysed at any age across all biospecimens analysed. Therefore, our results suggest that TDO may more likely drive the increased Trp metabolization through the KP.

Existing studies on the role of both these enzymes (TDO and IDO) in Trp metabolism are conflicting. Initially, the main enzyme responsible for the conversion of Trp to KYN under a range of pathological conditions was assumed to be IDO, while the role of TDO was restricted to physiological situations.[59] Interestingly, IDO has also been implicated in a rat model of renal fibrosis subjected to unilateral ureteral obstruction though TDO status was not studied in that model.[60] IDO activity has also been associated with chronic kidney disease and psychological/cognitive disease.[61]

Conversely, there are studies that report increased TDO in rats with chronic renal insufficiency, but no change in IDO levels.[42,46] According to these studies, some key factors in TDO induction could be the increased levels of glucagon and/ or glucocorticosteroids, whose levels increase during the course of renal failure and uremia. These can act as endogenous activators of TDO.[46,62,63] These putative TDO inductors were not analysed in the present study. Tankiewicz et al. studied TDO and IDO activity in liver and kidney tissue samples from rats with end-stage chronic kidney disease.[52] They report a decrease in Trp and increase in KYN levels in plasma as well as kidney tissues, which were attributed to the increased TDO activity observed in liver of diseased rats. Similarly, Pawlak et al. reported that liver TDO activity is enhanced in rats with experimental chronic renal failure, whereas IDO activity in extrahepatic tissues remained unchanged. Therefore, while the literature indicates varied reports of TDO or IDO as underlying linchpins for Trp metabolism in cohorts with chronic renal disease, our study on the LPK rat indicate Trp metabolism via KP through TDO activation due to the lack of accumulated neopterin.

Considering the biological function of IDO and its role in diseases[64], it might seem surprising we did not find an increased activity of this enzyme in a model of PKD that presents with renal fibrosis, inflammation, reduced renal function and evidence of uremia[13]. Perhaps the hypothesis proposed by Tankiewicz et al., could shed some light into the complexities of the feedback mechanisms governing the KP in chronic kidney diseases under such an immune response.[65] Specifically, Tankiewicz et al. hypothesize that the rise in concentration of interferon-γ (INF- γ) in individuals with chronic kidney diseases could lead to an induction of IDO as well as nitric oxide (NO) synthase.[52] However, NO synthase (NOS) activity would in turn facilitate a rise in NO levels which bears an affinity for the heme moiety in IDO, thereby decreasing its activity.[65-67] Huang et al. detected iNOS in cystic epithelial cells, stromal cells and macrophages, providing a physiological premise for further investigation into this pathway and its link to KP metabolites, especially because BH4 is a mandatory cofactor for all isoforms of NOS including iNOS.[68,69]

ii. With regards to a temporal increase in KP metabolites, this agrees with previously published studies that show increased KP metabolites in blood and peripheral tissues from patients and animal models with renal disease.[42-47] Taylor et al used the *jck* model of PKD with a Nek8 mutation and reported a decrease across 5 metabolites associated with Trp metabolism; Trp itself, indole-3-lactate, indole-3-acetate, 3-hydroxy-3-indoleacetic, and 2-ketoadipic acid.[25] In contrast to the current study, Abbiss et al detected Trp in 16-week kidney

tissue samples of LPK rats but did not detect Trp in Lewis control animals.[27] The cause of this discrepancy between our and the Abbiss et al dataset is unclear but might be a result of methodological differences. We suspect the absence of kidney Trp observed by Abbis et al could be due to the non-targeted method applied in their study.

The significant decrease in Trp in LPK rats at week-12 compared to Lewis controls is in line with other reports, which demonstrate similar changes in the concentration of this amino acid in the blood from patients with uremia and animal models of chronic renal insufficiency.[70,71] Several putative mechanisms of this aminoacidopathy have been proposed, including diminished intake of Trp with food.[72] The blood concentration of Trp depends on its supply with food, the activity of specific enzymes as well as its urine elimination.[42,70] Although changes in food intake were not assessed in the present study, the animals had permanent, unlimited access to granulated food and tap water. Furthermore, a reduced supply of a substrate normally results in a proportional reduction of its product, therefore, a decreased Trp supply would imply a decrease in KYN concentration. However, our results clearly demonstrate an overall increase in KYN and/or KP metabolite levels in kidney and plasma from LPK rats at week-12. Therefore, we propose that the decrease in the Trp levels in the LPK model is due to the increased metabolization of this amino acid through KP pathway.

The chief metabolite of the KP that is, KYN, can be metabolized to several downstream metabolites depending on the expression of KP enzymes and their activity within a given tissue or cell type. The kidneys have a substantial influence on KP metabolism due to their abundant expression of KP enzymes. Specifically, kidney tissue uptakes KYN and its metabolite 3-HK from circulating blood, and after metabolism, excretes them in the form of KYNA and XA respectively.[41] Circulating levels of 3-HK, XA and KYNA was found to be substantially elevated in 12-week LPK animals. Furthermore, we observed a significant increase in the levels of KYN in the 12-week LPK kidney which was in accordance with the trend of circulating KYN in 12-week LPK plasma. Similar results were observed in an animal model of renal insufficiency that showed KP metabolite excretion in urine despite decline in renal function.[42] The main route of eliminating KP metabolites is urine,[40] however we did not observe any significant change in the levels of KP metabolites in the urine, with the exception of decreased KYN in the urine of LPK animals, that could be attributed to renal impairment observed in these animals that changed with disease progression. It must be noted however, that failure to excrete KP metabolites would evidently lead to its accumulation in tissues and circulation which has been proposed to result in uremic syndromes.[46] This has been demonstrated in this study using the LPK model as well, wherein we observe an elevation of KP metabolites in the plasma but lack of

significant changes in metabolites (excepting KYN) in the urine. Therefore, the decrease in Trp along with increase in KP metabolites observed in the LPK rats is suspected to be a result of increased KP enzyme activity with no proportional increase in KP metabolite elimination. Increased activity of the KP enzymes alongside decreased KP metabolite excretion is reflected by increased levels of KP metabolites in the kidney and in the circulation.

In the present study, the urine was collected from the animals using metabolic cages while the tissue samples were collected after animal euthanasia. In terms of translatability if considering collection and analysis of comparable human samples, the urine samples can be considered as the most comparable biomarker source as it was collected from free moving unrestrained animals during the course of the study. In comparison, blood was collected immediately after euthanasia using a high dose of anesthetic agent. This will have had potential impact causing likely some variation from samples collected in an unanesthetized and unrestrained state. The kidney tissue samples could be compared to human samples collected via biopsy in humans but we acknowledge such samples are much harder to acquire and therefore not as translatable into clinical study or practice. However, it is worthy to note that levels of the KP metabolites in these 3 different biospecimens contribute to the understanding of not only the local but also the systemic KP metabolism status. For example, the combination of KP metabolites levels in urine and plasma can provide an indication of the renal function, given the fact that the main route of elimination of KYN and its metabolites is renal excretion and renal impairment may result in accumulation of KP metabolites in urine and/or plasma.[40] Therefore, the information about the simultaneous KP metabolites levels in these different biospecimens are important as they provide complementary information about KP metabolism in a pathological condition such as cystic kidney disease.

Trp was the only compound observed to be different between LPK rats and age matched Lewis controls in more than 1 biospecimen, that is, kidney and plasma. This observation suggests that Trp may be a good marker for kidney dysfunction. However, it is important to note that under normal conditions Trp alteration may result from increased metabolization of this amino acid through the KP (being the main route for Trp metabolisation).[31] Trp levels also depend on its supply with food, the activity of specific enzymes as well as its urine elimination.[42,70] There is therefore a myriad of factors that would need to be considered once a dysregulation of Trp is observed. The analysis of a group of KP metabolites as biomarkers, as performed in the present study, provides information about Trp fate, that is, whether Trp is being metabolized through the KP or not.

In summary, the increased levels of KP metabolites in our LPK model can be hypothesized to be due to the activation of the rate-limiting enzyme TDO governing the metabolism of Trp though the KP. The renal impairment in the LPK model with progression of the disease could be attributed to the accumulation of metabolites of this pathway in the peripheral circulation and body tissues. Indirect estimation of KP enzymes (such as TDO, IDO, KMO, KATs) showed diverse temporal profiles in the LPK rats across the various biospecimens studied. Whether these changes were driven through enhanced expression of enzymes responsible for the biogenesis of metabolites and/or accumulation of the metabolites due to progressive renal impairment is difficult to predict without monitoring the expression of the enzymes. Dedicated studies on Trp supplementation and the effect of accumulation of individual KP metabolites such as KYN, XA, 3-HK, and 3-HAA are required to further understand their role in the pathobiology of PKD as observed in LPK rats. Future investigations on upstream drivers responsible for Trp metabolism including effect of both IDO and TDO alongside KP metabolite regulation in our LPK model may shed light into the intricate processes governing PKD pathobiology and may build the foundation for exploring novel therapeutic alternatives in the treatment of genetic cystic kidney diseases.

Conclusion

Our research demonstrates an up-regulation of the KP, given the temporal increase of KP metabolite levels in kidney and plasma alongside no significant changes in these metabolites in urine, the main route of KP metabolite elimination. These results suggest that activation of the KP might be involved in the pathophysiology of the renal impairment observed in LPK rat model of PKD. Our research and others' data encourage further studies exploring the role of KP metabolites in cystic kidney diseases.

Study Limitations

The present study has some limitations that should be considered. First, we did not directly measure enzymatic activity of TDO, IDO, and downstream KP enzymes. Our study evaluated IDO/TDO activity indirectly by estimating the plasma KYN to Trp ratio. Such an approach does not consider the low circulating Trp levels that may arise from malnutrition, or decreased renal excretion of KP products.[58] Future studies could target direct measurement of enzymes responsible for conversion of metabolites to validate these findings. A second limitation of this study was that the food intake was not measured. Decrease of food intake is not an unusual outcome in chronic kidney disease animal models and it can be reflected in changes of Trp levels.[72] Additionally, the biospecimens for this study were obtained from archival samples therefore plasma, kidney and urine for each strain/age/sex cohort are not necessarily from the same groups of animals. We acknowledge that such limitation can increase the margin of error and reduce the power of the study. Although a minimum $n = 5$ for each group

of biospecimens were obtained from archival samples and attempts were made to sex match all the biospecimens across the groups, this was not achieved in all cases due to archival tissue sample availability. Considering that sex hormones can affect the activity of some KP enzymes and that KP metabolite associations are reported to be distinct for females and males,[73] sex is an important consideration in both the analysis and interpretation of the data. Sex effects were therefore analyzed in the statistical methods, but sex related differences for the KP metabolites were not identified. However, we acknowledge that a larger sample size may have highlighted these differences. Future studies should be conducted including matched biospecimens from the same animal as well as sufficient female and male cohorts in order to evaluate sex-related differences. The present study therefore provides a strong foundation for future work that could incorporate further control of these variables and direct measurement of KP enzymes to strengthen these findings.

Supplemental Material
Supplemental material for this article is available online.

REFERENCES

1. Bergmann C, Guay-Woodford LM, Harris PC, Horie S, Peters DJM, Torres VE. Polycystic kidney disease. *Nat Rev Dis Primers*. 2018;4:50.
2. Hildebrandt F. Genetic kidney diseases. *Lancet*. 2010;375:1287-1295.
3. Bergmann C. Genetics of autosomal recessive polycystic kidney disease and its differential diagnoses. *Front Pediatr*. 2017;5:221.
4. Hildebrandt F, Zhou W. Nephronophthisis-associated ciliopathies. *J Am Soc Nephrol*. 2007;18:1855-1871.
5. Hurd TW, Hildebrandt F. Mechanisms of nephronophthisis and related ciliopathies. *Nephron Exp Nephrol*. 2011;118:e9-14.
6. Vanholder R, Baurmeister U, Brunet P, Cohen G, Glorieux G, Jankowski J. A bench to bedside view of uremic toxins. *J Am Soc Nephrol*. 2008;19:863-870.
7. Torres VE, Chapman AB, Devuyst O, et al. Tolvaptan in patients with autosomal dominant polycystic kidney disease. *New Engl J Med*. 2012;367:2407-2418.
8. U.S. Food and Drug Administration. *Drug Approval Package: Jynarque (tolvaptan)*. 2018. Accessed September 2, 2022. https://www.accessdata.fda.gov/drugsatfda_docs/nda/2018/204441Orig1s000TOC.cfm
9. Braun DA, Hildebrandt F. Ciliopathies. *Cold Spring Harb Perspect Biol*. 2017;9:1-28.
10. Srivastava S, Molinari E, Raman S, Sayer JA. Many genes-one disease? Genetics of nephronophthisis (NPHP) and NPHP-associated disorders. *Front Pediatr*. 2017;5:287.
11. Otto EA, Trapp ML, Schultheiss UT, Helou J, Quarmby LM, Hildebrandt F. NEK8 mutations affect ciliary and centrosomal localization and may cause nephronophthisis. *J Am Soc Nephrol*. 2008;19:587-592.
12. Atala A, Freeman MR, Mandell J, Beier DR. Juvenile cystic kidneys (jck): a new mouse mutation which causes polycystic kidneys. *Kidney Int*. 1993;43:1081-1085.
13. Phillips JK, Hopwood D, Loxley RA, et al. Temporal relationship between renal cyst development, hypertension and cardiac hypertrophy in a new rat model of autosomal recessive polycystic kidney disease. *Kidney Blood Press Res*. 2007;30:129-144.
14. McCooke JK, Appels R, Barrero RA, et al. A novel mutation causing nephronophthisis in the Lewis polycystic kidney rat localises to a conserved RCC1 domain in nek8. *BMC Genomics*. 2012;13:393.
15. Menezes LF, Germino GG. The pathobiology of polycystic kidney disease from a metabolic viewpoint. *Nat Rev Nephrol*. 2019;15:735-749.
16. Padovano V, Podrini C, Boletta A, Caplan MJ. Metabolism and mitochondria in polycystic kidney disease research and therapy. *Nat Rev Nephrol*. 2018;14:678-687.
17. Priolo C, Henske EP. Metabolic reprogramming in polycystic kidney disease. *Nat Med*. 2013;19:407-409.
18. Rowe I, Chiaravalli M, Mannella V, et al. Defective glucose metabolism in polycystic kidney disease identifies a new therapeutic strategy. *Nat Med*. 2013;19:488-493.
19. Sánchez-López E, Kammeijer GSM, Crego AL, et al. Sheathless CE-MS based metabolic profiling of kidney tissue section samples from a mouse model of polycystic kidney disease. *Sci Rep*. 2019;9:806.
20. Menezes LF, Zhou F, Patterson AD, et al. Network analysis of a Pkd1-mouse model of autosomal dominant polycystic kidney disease identifies HNF4α as a disease modifier.. *PLoS Genet*. 2012;8:e1003053.
21. Menezes LF, Lin CC, Zhou F, Germino GG. Fatty acid oxidation is impaired in an orthologous mouse model of autosomal dominant polycystic kidney disease. *EBioMedicine*. 2016;5:183-192.
22. Gronwald W, Klein MS, Zeltner R, et al. Detection of autosomal dominant polycystic kidney disease by NMR spectroscopic fingerprinting of urine. *Kidney Int*. 2011;79:1244-1253.
23. Toyohara T, Suzuki T, Akiyama Y, et al. Metabolomic profiling of the autosomal dominant polycystic kidney disease rat model. *Clin Exp Nephrol*. 2011;15:676-687.
24. Hwang VJ, Kim J, Rand A, et al. The cpk model of recessive PKD shows glutamine dependence associated with the production of the oncometabolite 2-hydroxyglutarate. *Am J Physiol Renal Physiol*. 2015;309:F492-F498.
25. Taylor SL, Ganti S, Bukanov NO, et al. A metabolomics approach using juvenile cystic mice to identify urinary biomarkers and altered pathways in polycystic kidney disease. *Am J Physiol Renal Physiol*. 2010;298:F909-F922.
26. Abbiss H, Maker GL, Gummer J, et al. Development of a non-targeted metabolomics method to investigate urine in a rat model of polycystic kidney disease. *Nephrology*. 2012;17:104-110.
27. Abbiss H, Maker GL, Gummer JPA, et al. Untargeted gas chromatography-mass spectrometry-based metabolomics analysis of kidney and liver tissue from the Lewis polycystic kidney rat. *J Chromatogr B Analyt Technol Biomed Life Sci*. 2019;1118-1119:25-32.
28. Le Floc'h N, Otten W, Merlot E. Tryptophan metabolism, from nutrition to potential therapeutic applications. *Amino Acids*. 2011;41:1195-1205.
29. Grahame-Smith DG. The biosynthesis of 5-hydroxytryptamine in brain. *Biochem J*. 1967;105:351-360.
30. Heuther G, Hajak G, Reimer A, et al. The metabolic fate of infused L-tryptophan in men: possible clinical implications of the accumulation of circulating tryptophan and tryptophan metabolites. *Psychopharmacology*. 1992;109:422-432.
31. Schröcksnadel K, Wirleitner B, Winkler C, Fuchs D. Monitoring tryptophan metabolism in chronic immune activation. *Clin Chim Acta*. 2006;364:82-90.
32. Saito K, Crowley JS, Markey SP, Heyes MP. A mechanism for increased quinolinic acid formation following acute systemic immune stimulation. *J Biol Chem*. 1993;268:15496-15503.
33. Beadle GW, Mitchell HK, Nyc JF. Kynurenine as an intermediate in the formation of nicotinic acid from tryptophane by neurospora. *Proc Natl Acad Sci U S A*. 1947;33:155-158.
34. Wolf H. The effect of hormones and vitamin B6 on urinary excretion of metabolites of the kynurenine pathway. *Scand J Clin Lab Invest*. 1974;136:1-186.
35. Hilmas C, Pereira EF, Alkondon M, Rassoulpour A, Schwarcz R, Albuquerque EX. The brain metabolite kynurenic acid inhibits alpha7 nicotinic receptor activity and increases non-alpha7 nicotinic receptor expression: physiopathological implications. *J Neurosci*. 2001;21:7463-7473.
36. Ganong AH, Cotman CW. Kynurenic acid and quinolinic acid act at N-methyl-D-aspartate receptors in the rat hippocampus. *J Pharmacol Exp Ther*. 1986;236:293-299. 0022-3565 (Print).
37. Braidy N, Grant R, Adams S, Brew BJ, Guillemin GJ. Mechanism for quinolinic acid cytotoxicity in human astrocytes and neurons. *Neurotox Res*. 2009;16:77-86.
38. Belladonna ML, Grohmann U, Guidetti P, et al. Kynurenine pathway enzymes in dendritic cells initiate tolerogenesis in the absence of functional IDO. *J Immunol*. 2006;177:130-137.
39. Lugo-Huitrón R, Blanco-Ayala T, Ugalde-Muñiz P, et al. On the antioxidant properties of kynurenic acid: free radical scavenging activity and inhibition of oxidative stress. *Neurotoxicol Teratol*. 2011;33:538-547.
40. Holmes EW. Determination of serum kynurenine and hepatic tryptophan dioxygenase activity by high-performance liquid chromatography. *Anal Biochem*. 1988;172:518-525.
41. Takeuchi F, Tsubouchi R, Izuta S, Shibata Y. Kynurenine metabolism and xanthurenic acid formation in vitamin bB6-deficient rat after tryptophan injection. *J Nutr Sci Vitaminol*. 1989;35:111-122.
42. Saito K, Fujigaki S, Heyes MP, et al. Mechanism of increases in L-kynurenine and quinolinic acid in renal insufficiency. *Am J Physiol Renal Physiol*. 2000;279:F565-F572.
43. Schefold JC, Zeden JP, Fotopoulou C, et al. Increased indoleamine 2,3-dioxygenase (IDO) activity and elevated serum levels of tryptophan

catabolites in patients with chronic kidney disease: a possible link between chronic inflammation and uraemic symptoms. *Nephrol Dial Transplant*. 2009;24:1901-1908.

44. Pawlak D, Pawlak K, Malyszko J, Mysliwiec M, Buczko W. Accumulation of toxic products degradation of kynurenine in hemodialyzed patients. *Int Urol Nephrol*. 2001;33:399-404.

45. Pawlak K, Kowalewska A, Mysliwiec M, Pawlak D. Kynurenine and its metabolites–kynurenic acid and anthranilic acid are associated with soluble endothelial adhesion molecules and oxidative status in patients with chronic kidney disease. *Am J Med Sci*. 2009;338:293-300.

46. Pawlak D, Tankiewicz A, Matys T, Buczko W. Peripheral distribution of kynurenine metabolites and activity of kynurenine pathway enzymes in renal failure. *J Physiol Pharmacol*. 2003;54:175-189.

47. Pawlak D, Tankiewicz A, Buczko W. Kynurenine and its metabolites in the rat with experimental renal insufficiency. *J Physiol Pharmacol*. 2001;52:755-766.

48. Zhao J. Plasma kynurenic acid/tryptophan ratio: a sensitive and reliable biomarker for the assessment of renal function. *Ren Fail*. 2013;35:648-653.

49. Guillemin GJ, Cullen KM, Lim CK, et al. Characterization of the kynurenine pathway in human neurons. *J Neurosci*. 2007;27:12884-12892.

50. Staats Pires A, Tan VX, Heng B, Guillemin GJ, Latini A. Kynurenine and tetrahydrobiopterin pathways crosstalk in pain hypersensitivity. *Front Neurosci*. 2020;14:620.

51. Pawlak K, Brzosko S, Mysliwiec M, Pawlak D. Kynurenine, quinolinic acid–the new factors linked to carotid atherosclerosis in patients with end-stage renal disease. *Atherosclerosis*. 2009;204:561-566.

52. Tankiewicz A, Pawlak D, Topczewska-Bruns J, Buczko W. Kidney and liver kynurenine pathway enzymes in chronic renal failure. *Adv Exp Med Biol*. 2003;527:409-414.

53. Korstanje R, Deutsch K, Bolanos-Palmieri P, et al. Loss of kynurenine 3-monooxygenase causes proteinuria. *J Am Soc Nephrol*. 2016;27:3271-3277.

54. Pawlak D, Tankiewicz A, Mysliwiec P, Buczko W. Tryptophan metabolism via the kynurenine pathway in experimental chronic renal failure. *Nephron*. 2002;90:328-335.

55. Badawy AA. Tryptophan availability for kynurenine pathway metabolism across the life span: control mechanisms and focus on aging, exercise, diet and nutritional supplements. *Neuropharmacol*. 2017;112:248-263.

56. Ott M, Litzenburger UM, Rauschenbach KJ, et al. Suppression of TDO-mediated tryptophan catabolism in glioblastoma cells by a steroid-responsive FKBP52-dependent pathway. *Glia*. 2015;63:78-90.

57. Yoshida R, Imanishi J, Oku T, Kishida T, Hayaishi O. Induction of pulmonary indoleamine 2,3-dioxygenase by interferon. *Proc Natl Acad Sci U S A*. 1981;78:129-132.

58. Badawy AA, Guillemin G. The plasma [kynurenine]/[tryptophan] ratio and indoleamine 2,3-dioxygenase: time for appraisal. *Int J Tryptophan Res*. 2019;12:1178646919868978.

59. Eleftheriadis T, Antoniadi G, Liakopoulos V, Stefanidis I, Galaktidou G. Plasma indoleamine 2,3-dioxygenase concentration is increased in hemodialysis patients and may contribute to the pathogenesis of coronary heart disease. *Ren Fail*. 2012;34:68-72.

60. Matheus LHG, Simão GM, Amaral TA, et al. Indoleamine 2,3-dioxygenase (IDO) increases during renal fibrogenesis and its inhibition potentiates TGF-β 1-induced epithelial to mesenchymal transition. *BMC Nephrol*. 2017;18:287.

61. Karu N, McKercher C, Nichols DS, et al. Tryptophan metabolism, its relation to inflammation and stress markers and association with psychological and cognitive functioning: Tasmanian Chronic Kidney Disease pilot study. *BMC Nephrol*. 2016;17:171.

62. Liu JJ, Liu S, Gurung RL, et al. Relationship between fasting plasma glucagon level and renal function-a cross-sectional study in individuals with type 2 diabetes. *J Endocr Soc*. 2019;3:273-283.

63. Walser M, Ward L. Progression of chronic renal failure is related to glucocorticoid production. *Kidney Int*. 1988;34:859-866.

64. Hornyák L, Dobos N, Koncz G, et al. The role of indoleamine-2,3-dioxygenase in cancer development, diagnostics, and therapy. *Front Immunol*. 2018;9:151.

65. Chiarugi A, Dello Sbarba P, Paccagnini A, Donnini S, Filippi S, Moroni F. Combined inhibition of indoleamine 2,3-dioxygenase and nitric oxide synthase modulates neurotoxin release by interferon-gamma-activated macrophages. *J Leukoc Biol*. 2000;68:260-266.

66. Thomas SR, Mohr D, Stocker R. Nitric oxide inhibits indoleamine 2,3-dioxygenase activity in interferon-gamma primed mononuclear phagocytes. *J Biol Chem*. 1994;269:14457-14464.

67. Law BMP, Wilkinson R, Wang X, et al. Interferon-γ production by tubulointerstitial human CD56bright natural killer cells contributes to renal fibrosis and chronic kidney disease progression. *Kidney Int*. 2017;92:79-88.

68. Huang XB, Ito F, Nakazawa H, et al. Inducible nitric oxide synthase localization in acquired cystic disease of the kidney. *Nephron*. 1999;81:360-361.

69. McNeill E, Crabtree MJ, Sahgal N, et al. Regulation of iNOS function and cellular redox state by macrophage Gch1 reveals specific requirements for tetrahydrobiopterin in NRF2 activation. *Free Radic Biol Med*. 2015;79:206-216.

70. Holmes EW, Kahn SE. Tryptophan distribution and metabolism in experimental chronic renal insufficiency. *Exp Mol Pathol*. 1987;46:89-101.

71. Holmes EW, Russell PM, Kinzler GJ, Bermes Ew Jr. Inflammation-associated changes in the cellular availability of tryptophan and kynurenine in renal transplant recipients. *Clin Chim Acta*. 1994;227:1-15.

72. Topczewska-Bruns J, Tankiewicz A, Pawlak D, Buczko W. Behavioral changes in the course of chronic renal insufficiency in rats. *Pol J Pharmacol*. 2001;53:263-269.

73. Oluwagbemigun K, Anesi A, Clarke G, Schmid M, Mattivi F, Nöthlings U. An investigation into the temporal reproducibility of tryptophan metabolite networks among healthy adolescents. *Int J Tryptophan Res*. 2021;14:11786469211041376.